Computers in Biology and Medicine 90 (2017) 15–22

Contents lists available at ScienceDirect

Computers in Biology and Medicine

journal homepage: www.elsevier.com/locate/compbiomed

A mechanistic model for drug release from PLGA-based drug eluting stent: A computational study

Jahed Naghipoor *, Timon Rabczuk

Chair of Computational Mechanics, Institute of Structural Mechanics, Bauhaus University of Weimar, 99423, Weimar, Germany

ARTICLE INFO

Keywords:
PLGA-based bioabsorbable stent
Viscoelasticity
Numerical simulation

ABSTRACT

Atherosclerosis in the coronary artery is one of the leading causes of death in the world. The stenting as a minimally invasive technique was considered as an effective tool to reduce the severity of atherosclerotic stenosis. In-stent restenosis is the main drawback of the stenting in the coronary artery. Understanding the mechanism of drug release from drug-eluting stents and drug uptake in the arterial wall and obtaining more information about their functionality using mathematical modeling and numerical simulation, could be considered as a predictive tool to investigate in-stent restenosis growth which is experimentally expensive to study. In this work, the local delivery of a therapeutic agent from a PLGA-based bioabsorbable stent implanted in a coronary artery to predict the drug release as well as spatio-temporal drug distribution in a coronary artery with a vulnerable plaque is mathematically modeled and numerically simulated. The effect of copolymer ratio on drug release has been also investigated.

1. Introduction

Atherosclerosis is one of the most serious and common forms of cardiovascular disease which arises due to the accumulation of fatty deposits, cholesterol and calcified material in the arterial wall. It gradually occludes the lumen and reduces the blood flow [1].

Surgical techniques such as coronary artery bypass graft (CABG) and percutaneous coronary intervention (PCI) are techniques to reduce the severity of the advanced atherosclerotic stenosis in the coronary artery. Balloon angioplasty was considered as a less invasive intervention to open up the occluded lumen. Clinical observations indicate that balloon angioplasty is highly associated with restenosis [2,3].

The emergence of bare metal stents (BMS) has revolutionized the balloon angioplasty procedure by reducing the possibility of restenosis. While BMS had the standard of care for atherosclerosis for decades, they present a major shortcoming due to the relatively quick occurrence of the in-stent restenosis, that is the re-narrowing of the lumen, as a result of wounded endothelial cells proliferation caused by stent implantation. The next generation of arterial stents, drug-eluting stent (DES), was invented to overcome in-stent restenosis after BMS implantation [4]. The therapeutic effects of DES together with its mechanical scaffolding have proposed promising benefits to reduce in-stent restenosis compared to BMS [5,6].

Atherosclerosis mainly affects the intima, but the media which is the thickest arterial layer could be also affected in the advanced stages. This alteration introduces a significant change in the mechanical properties of the arterial wall. Mechanical behavior of the atherosclerotic regions in the coronary artery differs significantly from the healthy one [7]. During the last years, mathematical models have been studied by several authors for coupled drug delivery in the cardiovascular tissues. We refer without being exhaustive to [8–15]. Most of these studies address the release of the drug while the mechanical properties of the arterial wall are disregarded. To include the mechanical properties of the arterial wall, a non-Fickian reaction-diffusion-convection model is developed by some of the authors [16–18].

PLGA, the linear copolymer of polylactic acid and polyglycolic acid, has been widely used in drug delivery devices due to its biocompatibility and tailored biodegradation rate. A number of PLGA-based biodegradable stents including Xinsorb BRS, Hua'an and DREAMS I, Biotronik, have been developed in recent years [19]. Depending on the ratio of lactide to glycolide used for the polymerization, different forms of PLGA can be obtained where the rate of drug release from PLGA-based stents would likely depend on the copolymer ratio [20,21].

In this paper, we study the integrated effect of the mechanical properties of the arterial wall and degradation mechanism of polymer on the release of drug from PLGA-based bioabsorbable stent into the arterial

* Corresponding author.
E-mail address: jahed.naghipoor@uni-weimar.de (J. Naghipoor).

http://dx.doi.org/10.1016/j.compbiomed.2017.09.001
Received 6 June 2017; Received in revised form 1 September 2017; Accepted 1 September 2017

Table 1
Notations in the stent (S), healthy wall (H), plaque (P) and fibrous cap (FC).

	Fluid	Polymer	Monomer	Solid drug	Dissolved drug	Bound drug	Unbound drug
S	*W*	*P*	*m*	*SD*	*DD*	–	–
H	*W*	–	*m*	–	–	*BD*	*UD*
P	*W*	–	*m*	–	–	*BD*	*UD*
FC	*W*	–	*m*	–	–	*BD*	*UD*

wall. We will study the effect of copolymer ratio on the drug release and polymer degradation.

The paper is organized as follows. In Section 2, we provide details of a mathematical model which includes mechanical and chemical ingredients of a PLGA-based stent and the arterial wall respectively. Section 3 is devoted to the numerical simulations of drug release from stent into arterial wall. We conclude the paper with some conclusions and suggestion in the last section.

2. Mathematical modeling

Let us consider a two-dimensional domain in the longitudinal direction containing a PLGA-based bioabsorbable stent (S) with an impermeable metallic core, the plaque (P), the fibrous cap (FC) and the healthy part of the arterial wall (H). The plaque is composed of fatty laden foam cells and fibrous cap mainly consists of proliferated smooth muscle cells. The diseased condition is designed by incorporating geometric and structural modifications caused by the progression of atherosclerosis like lipid accumulation, intima thickening, and fibrous cap formation while keeping the transport properties for the unaltered layers (the healthy part of the arterial wall). For a sake of simplicity, we consider that stent is partially embedded in the fibrous cap which is a simplification with respect to the complex dynamics of tissue healing and regrowth that takes place after stent implantation. As a comparative study of different configurations of the physical parameters characterizing the stent are of interests, the evolution of neointima around the stent can be initially neglected [13,22].

This work presents a mathematical model that describes the integrated process of drug release in PLGA coating and subsequent drug distribution in the arterial wall. A mechanistic model for the drug release in the PLGA coating is considered which couples the drug diffusion to the PLGA degradation. The model is integrated with the viscoelastic properties of the arterial wall. The drug pharmacokinetics in the arterial wall is modeled as a reversible binding process. The mathematical model presented in this paper includes the following integrated items:

- Interaction between solid and dissolved drugs in the polymer;
- Degradation-dependent porosity of the polymer;
- Distribution of unbound and bound drugs in different regions of the arterial wall;
- The stiffness of the atherosclerotic plaque.

The following assumptions are taken into consideration in the mathematical model:

- Viscoelastic properties of the polymeric stent are considered negligible;
- Permeability and viscosity of the arterial wall are considered constants;
- Solid and dissolved drugs do not react with PLA and its reaction products;
- The mechanical stress due to stent implantation exists are not considered.

The main limitation of this study is the lack of appropriate experimental data. So the numerical results are not compared with experiments.

2.1. The mathematical model of the polymeric stent

We consider the notation $\mathscr{M}_S = \{W, P, m, SD, DD\}$, where *W*, *P*, *m*, *SD*, and *DD* stand for fluid, polymer, monomer, solid and dissolved drugs respectively.

The model presented here involves the diffusion of fluid, monomer, and drug through the polymeric matrix. Fluid enters from the polymer's boundaries and interacts with the polymer to produce oligomers and consequently monomers. Due to the low diffusivity of oligomers, only the diffusion of monomers was considered in this work. In Table 1, we summarize the previous notations.

Drug dissolution: As mentioned in Ref. [23], the drug release from a polymeric matrix is mainly influenced by dissolution of the drug and diffusion in the pores filling liquid. In most of the cases, the matrix systems are stored without any liquid phase inside. In this condition, the drug in the dry polymeric network cannot diffuse through the network meshes. Upon contact with the physiological fluid, the polymer swells and drug dissolution can take place. When the physiological fluid diffuses through the polymeric matrix via matrix boundaries, it activates the polymer swelling and the solid drug particles are then activated by fluid. The solid drug in contact with fluid starts to dissolve and finally the dissolved drug diffuses through the polymer matrix via degradation-controlled release [24]. The process is schematically modeled by the following relation:

$$C_{SD,S} \xrightarrow{\kappa_{DD,S}} C_{DD,S}, \tag{1}$$

where $C_{SD,S}$ and $C_{DD,S}$ stand for the concentrations of the solid drug (*SD*) and the dissolved drug (*DD*) respectively and $\kappa_{DD,S}$ is the dissolved coefficient.

Polymer degradation: Degradation alters the molecular weight and porosity of the polymer, and consequently alters the diffusivity of the dissolved drug in the polymer [22]. The effective diffusivity of dissolved drug in the polymer is defined as follows:

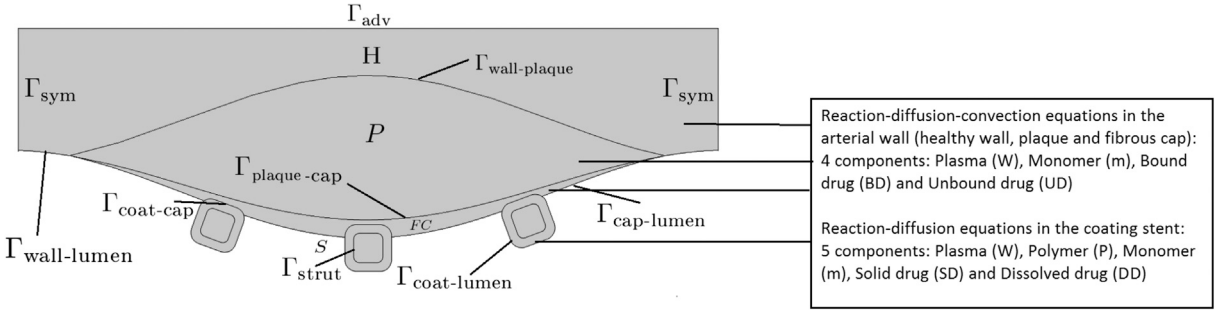

Fig. 1. Geometric representation of the longitudinal section.

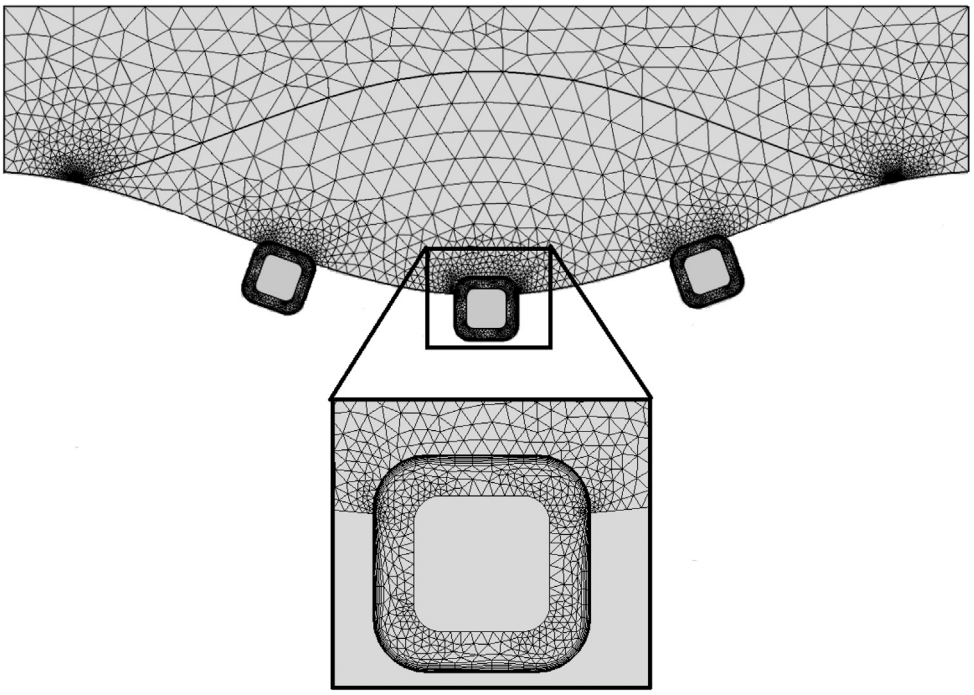

Fig. 2. Computational meshes in the domain.

$$D_{eff} = \frac{(1-\phi_S)D^0_{DD,S}e^{\alpha k_P t} + k_S\phi_S D_{UD,FC}}{1-\phi_S+k_S\phi_S}, \tag{2}$$

where $D^0_{DD,S}$ represents the initial diffusivity of drug in the solid part of the polymer, k_P is the degradation rate, $D_{UD,FC}$ stands for the diffusivity of the drug in the liquid-filled pores (the coating is in direct contact with the fibrous cap, Fig. 1), ϕ_S is the porosity of the polymer and k_S is drug partitioning between the liquid-filled pores and solid part of the polymer. Porosity in the polymer is formulated by the following formulation [22].

$$\phi_S = \phi_{S,0} + \left(1-\phi_{S,0}\right)\left(1+e^{-2k_P t} - 2e^{-k_P t}\right), \tag{3}$$

assuming the same density for the polymer of different lengths, where $\phi_{S,0}$ is the initial porosity in the PLGA. It is obvious that in $t = 0$, no erosion happened while at the end of the process polymer is completely eroded.

Table 2
Values for the parameters in the stent coating, arterial wall and lumen.

Parameter/Variable	Definition	Value
	Stent coating (S)	
$D_{W,S}$	diffusion coefficient of fluid	10^{-8} cm^2/s
$D_{m,S}$	diffusion coefficient of monomer	10^{-10} cm^2/s
$D^0_{DD,S}$	diffusion coefficient of dissolved drug	3.1×10^{-12} cm^2/s
$k_{DD,S}$	dissolution rate	10^{-4} $mol/cm^2.s$
$\phi_{S,0}$	initial porosity	0
C_{Sol}	maximum solubility	3×10^{-4} mol/cm^2
κ_S	partitioning coefficient	10^{-4}
	Arterial wall ($j = H,P,FC$)	
p_{adv}	pressure in adventitia	30 $mmHg$
p_{lumen}	pressure in lumen	120 $mmHg$
τ_j	relaxation time	0.5 s
κ_j	Young's modulus of the arm	1 MPa
k_j	permeability of the arterial wall	10^{-15} cm^2
μ_j	viscosity of plasma	5×10^{-2} $g/cm.s$
$B_{max,j}$	density of free binding sites	0.366 mol/m^2

The mechanism of the drug release can be described through the following steps: Fluid enters the polymer matrix from its boundaries and diffuses throughout it. In the meantime, it participates in the polymer degradation reactions. It breaks n-long polymer chain in various different sites, producing two shorter m-long and $n-m$-long chains and ultimately leads to the monomer formation by repetition of the reactions [25]. The adopted kinetic scheme is the following:

$$C_{P_n,S} + C_{W,S} \rightarrow C_{P_m,S} + C_{P_{n-m},S}. \tag{4}$$

The drug dissolution and diffusion of species through the polymer coating are described by a system of coupled partial differential equations of the following form:

$$\begin{cases} \dfrac{\partial C_{W,S}}{\partial t} &= -\nabla.J(C_{W,S}) + \dfrac{k_P}{k_{eq}}C_{W,S}(M_S - C_{P,S}) - k_P C^2_{P,S}, \\ \dfrac{\partial C_{P,S}}{\partial t} &= \dfrac{k_P}{k_{eq}}C_{W,S}(M_S - C_{P,S}) - k_P C^2_{P,S}, \\ \dfrac{\partial M_S}{\partial t} &= 0, \\ \dfrac{\partial C_{m,S}}{\partial t} &= -\nabla.J(C_{m,S}) + \dfrac{k_P}{k_{eq}}C_{W,S}(C_{P,S} - C_{m,S}) - 2k_P C_{P,S}C_{m,S}, \\ \dfrac{\partial C_{DD,S}}{\partial t} &= -\nabla.J(C_{DD,S}) - \kappa_{DD,S}C_{SD,S}(C_{Sol} - C_{DD,S}), \\ \dfrac{\partial C_{SD,S}}{\partial t} &= \kappa_{DD,S}C_{SD,S}(C_{Sol} - C_{DD,S}), \end{cases} \tag{5}$$

in $S\times IR^+$, where M_S stands for the mass of polymer and

$$\begin{aligned} J(C_{DD,S}) &= -D_{eff}\nabla C_{DD,S}, \\ J(C_{i,S}) &= -D_i\nabla C_{i,S}, \quad i = W,m, \end{aligned} \tag{6}$$

are fluxes of transportable molecules in the polymer.

The reaction terms for polymer degradations $(5)_1$, $(5)_2$ and $(5)_4$ are adapted from Refs. [24] and [25], where k_P and k_{eq} stand for the

polymerization rate and the thermodynamic equilibrium constants for the polymerization reactions respectively.

Initial and boundary conditions: Equations (5) and (6) are completed with initial and boundary conditions. At the initial time $t = 0$, the drug is assumed to be entirely contained in the polymer with a uniform concentration in its solid state. The initial conditions in the coating are as follows:

$$C_{i,S}(0) = 0, \quad i = W, m, DD, \quad C_{i,S}(0) = C^0_{i,S}, \quad i = P, SD. \tag{7}$$

As the metallic part of the stent, Γ_{strut}, is impermeable to diffusible species present in the polymer, the no-flux condition $J\,(C_{i,S})$. $\eta_S = 0$, $i = W, m, DD$, holds for Γ_{strut}. Monomers and dissolved drug pass through $\Gamma_{\text{coat}-\text{cap}}$ and diffuse into different regions of the arterial wall. As the n-long polymer chain $C_{P,S}$ does not diffuse to outside of the matrix, no boundary condition is necessary for equation $(5)_2$. As diffusible molecules in the $\Gamma_{\text{coat}-\text{lumen}}$ are immediately washed out by blood flow, Dirichlet boundary condition $C_{i,S} = 0$, $i = m,DD$, is prescribed. As fluid enters to the polymer through $\Gamma_{\text{coat}-\text{lumen}}$, Dirichlet boundary condition $C_{W,S} = C_{W,out}$ is applied.

2.2. The mathematical model of the arterial wall

We consider the notation $\mathscr{M}_j = \{W, m, BD, UD\}, \quad j = H, P, FC$, where *BD* and *UD* stand for the bound and unbound drugs in the arterial wall. We now establish the model for drug transport in the arterial wall.

Metabolic reactions: Similar to [26–28], we assume the reversible nature of the bindings between the drug and specific sites inside the arterial wall. Bindings occur when drug and binding site hit each other due to diffusion forces and when the collision has the correct orientation and enough energy [26]. When binding has occurred, drug and binding site remain bound together for an amount of time depending on the affinity of the binding site and type of drug. After dissociation, the drug and the binding site are the same as they were before binding.

The drug-binding site reaction is schematically represented by

$$\text{Drug} + \text{Binding sites} \underset{\text{dissociation}}{\overset{\text{association}}{\rightleftarrows}} \text{Drug} - \text{binding complex}. \tag{8}$$

To define the mathematical kinetic model associated to (8), we assume that all the binding sites are equally accessible to the drug. We also assume that there are not states of partial binding which means the binding sites are either free or attached to the drug. It is also assumed that neither drug nor binding sites are altered by binding reactions.

The drug assumes two different states: the unbound state where drug diffuses and the bound state where drug attaches reversibly to specific sites inside the arterial wall. The concentration of unbounded drug in the regions of the arterial wall is represented by $C_{UD,j}$, $j = H,P,FC$, with initial concentration $C^0_{UD,j} = 0$, while $B_{\max,j}$ represents the density of free binding sites in the regions of the arterial wall. $C_{BD,j}$ represents the concentration of bound drug with initial concentration $C^0_{BD,j} = 0$. The drug-binding reaction is schematically represented by

$$C_{BD,j} \underset{\kappa_{u,j}}{\overset{\kappa_{b,j}}{\rightleftarrows}} C_{UD,j}, \tag{9}$$

where $\kappa_{b,j}$ is the association rate between drug and binding sites and $\kappa_{u,j}$ is the dissociation rate. The flux associated with the release of drug has three components: convective, diffusive and viscoelastic.

Convection: Drug transport in the arterial wall is affected by convection induced by plasma filtration in the tissue, activated by physiological transmural pressure gradients. Plasma velocity and pressure in the arterial wall are governed by Darcy's equation. Let u_j and p_j, $j = H,P,FC$,

Table 3
Values for the parameters in the healthy wall, the plaque and the fibrous cap.

Parameter	Definition	Healthy wall (H)	Plaque (P)	Fibrous cap (FC)
$D_{\sigma_j}\,[g/(cmsPa)]$	viscoelastic diffusivity	5×10^{-8}	1×10^{-8}	8×10^{-8}
$D_{W,j}\,[cm^2/s]$	diffusivity of fluid	1×10^{-8}	1×10^{-15}	1×10^{-8}
$D_{m,j}\,[cm^2/s]$	diffusivity of monomer	1×10^{-10}	1×10^{-15}	1×10^{-10}
$D_{UD,j}\,[cm^2/s]$	diffusivity of unbound drug	7.7×10^{-8}	1.4×10^{-13}	6.2×10^{-8}
$\kappa_{r,j}\,[MPa]$	Young's modulus	1.5	4.2	1.2
ϕ_j	porosity	0.61	0.5	0.8

are the velocity vector of the plasma and the pressure in different regions of the arterial wall respectively. We have the following system for pressure and velocity in the arterial wall:

$$\begin{cases} u_j = -\dfrac{k_j}{\mu_j}\nabla p_j, \;\; \nabla . u_j = 0 \;\; \text{in} j = H,P,FC, \\ p_H = p_P, \;\; p_V = p_{FC} \;\; \text{on}\, \Gamma_{\text{wall}-\text{plaque}} \cup \Gamma_{\text{plaque}-\text{cap}}, \\ \dfrac{k_H}{\mu_H}\nabla p_H . \eta_H = -\dfrac{k_j}{\mu_j}\nabla p_j . \eta_j, \;\; j = P, FC \;\; \text{on}\, \Gamma_{\text{wall}-\text{plaque}} \cup \Gamma_{\text{plaque}-\text{cap}}, \\ \nabla p_{FC} . \eta_{FC} = 0 \;\; \text{on}\, \Gamma_{\text{coat}-\text{cap}}, \\ u_H . \eta_H = 0, \;\; \text{on}\, \Gamma_{\text{sym}}, \\ p_H = p_{\text{adv}} \;\; \text{on}\, \Gamma_{\text{adv}}, \\ p_{FC} = p_{\text{lumen}} \;\; \text{on}\, \Gamma_{\text{lumen}-\text{cap}} \cup \Gamma_{\text{wall}-\text{lumen}}, \end{cases} \tag{10}$$

where μ_j, k_j, $j = H,P,FC$, represent viscosity and permeability in different arterial regions respectively.

Viscoelastic effect: Regarding the diffusive component of the flux, it is well-known that Fick's law does not represent an accurate description of the phenomenon due to the viscoelastic effect of the arterial wall. The arterial wall consists of elastin that is responsible for the elasticity and also smooth muscle cell and collagen in the media which exhibit the viscoelastic behavior of the artery. Experiments like *creep test* have demonstrated that the vascular tissue is viscoelastic [29–31]. It is accepted that in the presence of small vascular deformations, the linear viscoelastic models adequately capture the viscoelastic properties of the arterial wall [29].

The linear viscoelastic model (*Maxwell-Wiechert* model, [32]),

$$\frac{\partial \sigma_j}{\partial t} + \frac{1}{\tau_j}\sigma_j = -\frac{k_j \kappa_{r_j}}{\tau_j}\left(C_{i,j} + \tau_{\sigma_j}\frac{\partial C_{i,j}}{\partial t}\right), \quad \text{in}\, j \times \text{IR}^+, \quad j = H, P, FC, \tag{11}$$

used in Ref. [17], is introduces to capture the viscoelastic properties of the healthy wall, the plaque and the fibrous cap where $\tau_j = \frac{\lambda_j}{\kappa_j}$ and $\tau_{\sigma_j} = \lambda_j \frac{\kappa_j + \kappa_{r_j}}{\kappa_j \kappa_{r_j}}, \quad j = H, P, FC$. The constants κ_j, $j = H,P,FC$, represent Young's modulus of the Maxwell's arm in each arterial region while λ_j, $j = H,P,FC$, are their viscosities. As the plaque is stiffer than the fibrous cap and the healthy wall, we consider $\kappa_{r_{FC}} \le \kappa_{r_H} \le \kappa_{r_P}$.

Equation (11) defines one of the simplest linear viscoelastic models that simultaneously captures the effects of creep and stress relaxation.

The non-Fickian nonlinear reaction-diffusion-convection model in the arterial wall reads:

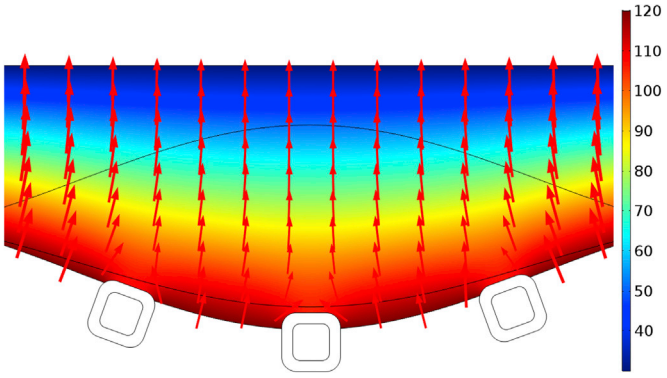

Fig. 3. Pressure [mmHg] and velocity field (only direction of the field is shown) in the stented arterial wall.

$$\begin{cases} \dfrac{\partial C_{W,j}}{\partial t} &= -\nabla . J\left(C_{W,j}\right), \\ \dfrac{\partial C_{m,j}}{\partial t} &= -\nabla . J\left(C_{m,j}\right), \\ \dfrac{\partial C_{UD,j}}{\partial t} &= -\nabla . J\left(C_{UD,j}\right) + \phi_j^{-1}\kappa_{u,j}C_{UD,j}\left(B_{max,j} - C_{BD,j}\right) - \kappa_{b,j}C_{BD,j}, \\ \dfrac{\partial C_{BD,j}}{\partial t} &= -\phi_j^{-1}\kappa_{u,j}C_{UD,j}\left(B_{max,j} - C_{BD,j}\right) + \kappa_{b,j}C_{BD,j}, \end{cases} \tag{12}$$

in $j \times \mathrm{IR}^+, j = H,P,FC$, where ϕ_j stands for the porosity in different regions of the arterial wall [33].

The mass flux in the arterial wall is defined by

$$J\left(C_{i,j}\right) = -\left(D_{i,j}\nabla C_{i,j} + D_{\sigma_j}\nabla\sigma_j - u_j C_{i,j}\right), \tag{13}$$

for $i \in \mathscr{M}_j, \quad j = H,P,FC,$ where u_j is the velocity field computed by Darcy's law using system (10) and σ_j is the stress component in each region computed by equation (11). D_{σ_j} represents the non-Fickian diffusion coefficient.

It is observed that the arterial wall is anisotropic and consequently diffusion has different values in transversal and longitudinal directions [34]. Thus, an anisotropic drug diffusivity is considered in (13) for diffusion of unbound drug in the arterial wall where the transversal vascular diffusivity is of one or two orders larger in the magnitude of longitudinal diffusion coefficient.

Initial, boundary and interface conditions: The model (12)–(13) are completed with initial, boundary and interface conditions. The following initial conditions are considered in different regions of the arterial wall:

$$C_{i,j}(0) = C_{i,j}^0, \quad i = W,BD, \quad C_{i,j}(0) = 0, \quad i = m,UD, \quad j = H,P,FC. \tag{14}$$

As the fluid penetrates from the lumen into the arterial wall, we consider a Dirichlet boundary condition $C_{W,j} = C_{W,out}$, $j = H,FC$, on $\Gamma_{\text{lumen}-\text{cap}} \cup \Gamma_{\text{wall}-\text{lumen}}$, where $C_{W,out}$ stands for the fluid concentration in the lumen. As monomers and unbound drug present in the arterial wall go directly to the bloodstream and are transported very fast away from the region of interest, the Dirichlet boundary condition $C_{i,j} = 0, i = UD,m,$

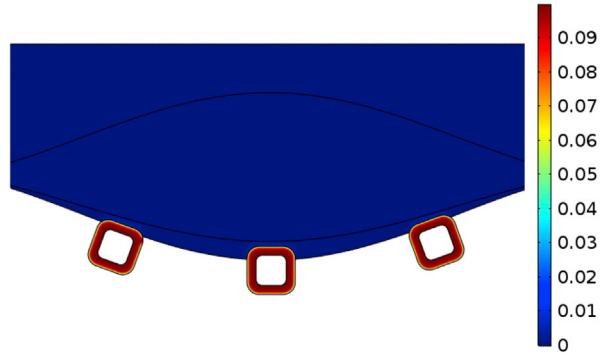

(a) Drug release, 1 day,

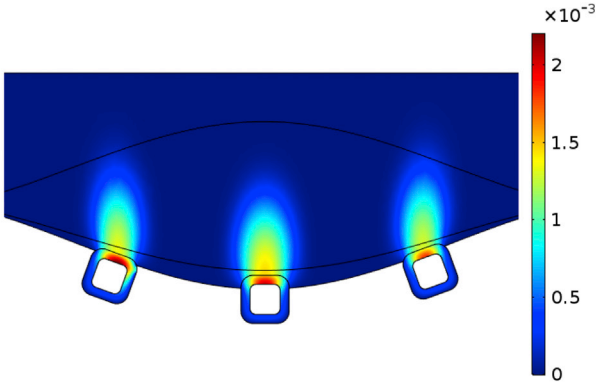

(b) Drug release, 90 days,

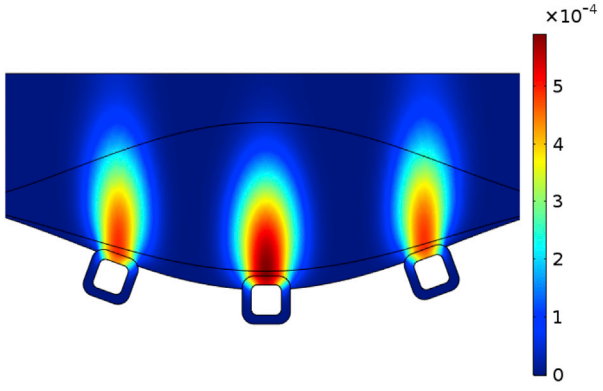

(c) Drug release, 180 days,

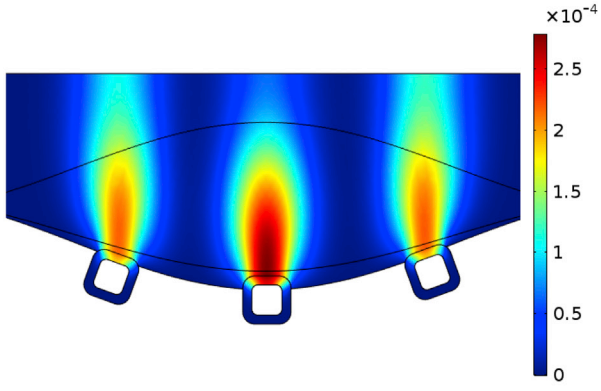

(d) Drug release, 360 days,

Fig. 4. Distribution of the drug $\left[\frac{mol}{cm^2}\right]$ during one year.

$j = H,FC$, is considered for these species on $\Gamma_{\text{lumen}-\text{cap}} \cup \Gamma_{\text{wall}-\text{lumen}}$. As adventitia is considered impermeable to all species present in the arterial wall, the no-flux condition $J(C_{i,H}).\eta_H = 0,\ i \in \mathscr{M}_H$, holds for Γ_{adv}.

The interface boundary conditions on $\Gamma_{\text{coat}-\text{cap}}$, $\Gamma_{\text{wall}-\text{plaque}}$ and $\Gamma_{\text{plaque}-\text{cap}}$ are as follows:

$$\begin{cases} C_{i,S} = C_{i,FC}, & \text{on } \Gamma_{\text{coat}-\text{cap}}, \\ J(C_{i,S}).\eta_S = -J(C_{i,FC}).\eta_{FC}, & \text{on } \Gamma_{\text{coat}-\text{cap}}, \end{cases} \tag{15}$$

for $i \in \mathscr{M}_{FC}$, $i \neq BD$,

$$\begin{cases} C_{i,H} = C_{i,P}, & \text{on } \Gamma_{\text{wall}-\text{plaque}}, \\ J(C_{i,H}).\eta_V = -J(C_{i,P}).\eta_P, & \text{on } \Gamma_{\text{wall}-\text{plaque}}, \end{cases} \tag{16}$$

for $i \in \mathscr{M}_P$, $i \neq BD$, and

$$\begin{cases} C_{i,P} = C_{i,FC}, & \text{on } \Gamma_{\text{plaque}-\text{cap}}, \\ J(C_{i,P}).\eta_P = -J(C_{i,FC}).\eta_{FC}, & \text{on } \Gamma_{\text{plaque}-\text{cap}}, \end{cases} \tag{17}$$

for $i \in \mathscr{M}_{FC}$, $i \neq BD$.

3. Numerical simulation

The governing equations are discretized in space by finite element method using the commercial software package COMSOL Multiphysics 5.1 (COMSOL AB, Burlington, MA, USA).

The stent coating and the arterial wall including the plaque and the fibrous cap are meshed as illustrated in Fig. 2, where a finer mesh in the coating is used considering the much smaller scale of the coating domain. Boundary layers are also imposed at the interface $\Gamma_{\text{coat}-\text{cap}}$ to improve the simulation accuracy. The time integration is backward differential formula (BDF). Piecewise quadratic finite element space P_2 for the concentrations and the pressure and piecewise linear finite element space P_1 for the velocity are used. The average mesh size of each stent, the healthy wall, the plaque, and the fibrous cap are $9.09 \times 10^{-3}m$ (1344 elements), $5.66 \times 10^{-7}m$ (9042 elements), $8.99 \times 10^{-7}m$ (4804 elements) and $1.47 \times 10^{-6}m$ (2198 elements) respectively. The computational time for the reference simulation performed on an Intel(R) Core(TM) i7-4790 3.60 GHz processor and 16.0 GB RAM is around 1 h. A convergence test has been done to ensure the adequate mesh density and validity of the simulation. The simulation is accomplished with two different mesh sizes to verify that the solution is convergent and mesh independent.

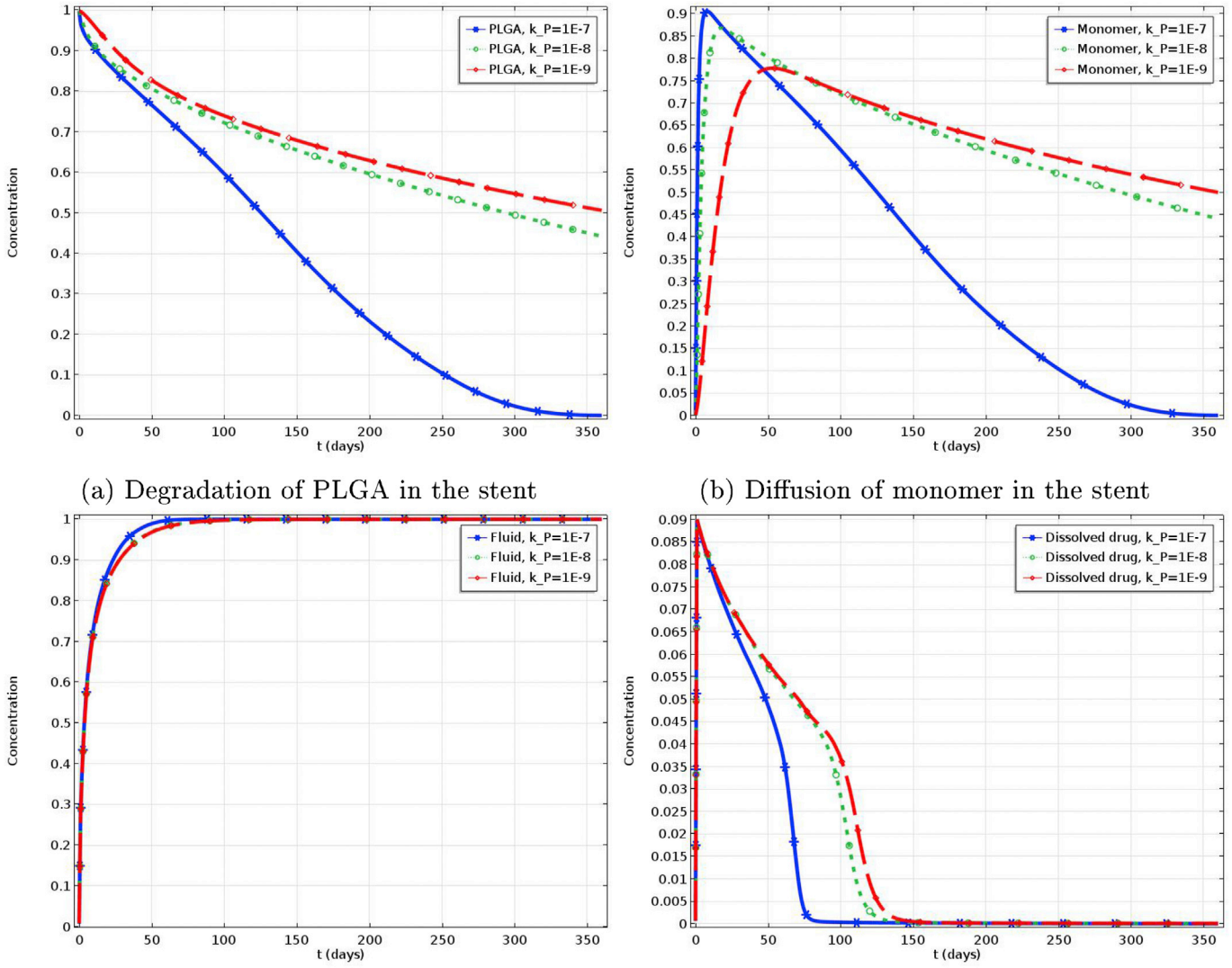

(a) Degradation of PLGA in the stent

(b) Diffusion of monomer in the stent

(c) Penetration of fluid in the stent,

(d) Diffusion of dissolved drug in the stent,

Fig. 5. Mean concentration of the species $\left[\frac{mol}{cm^2}\right]$; The effect of degradation rate on the release of species from stent.

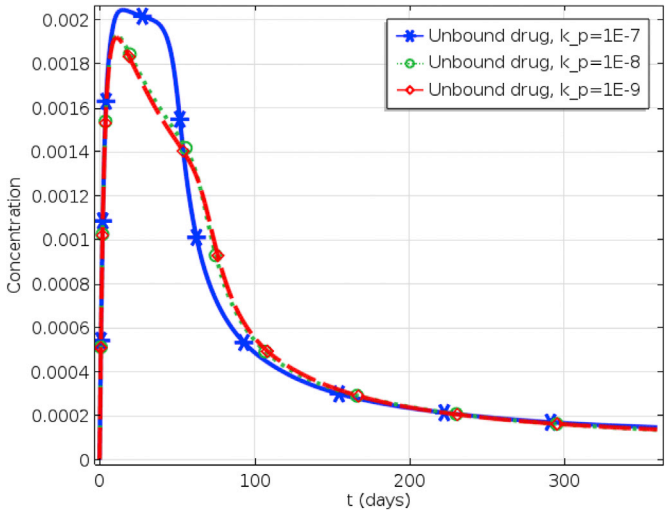

Fig. 6. Mean concentration of the unbound drug $\left[\frac{mol}{cm^2}\right]$; The effect of degradation rate on the diffusion of unbound drug in the arterial wall.

There is a large degree of variability in most parameters exhibited in the literature, due to the particular approach used in their estimation (as for example, in vivo vs. in vitro, human vs. animal). Parameters in Table 2 and Table 3 which have been extracted from Refs. [8–10,13,15,35,36] and [11], are used in all numerical experiments.

We study the mechanisms of the drug release from a PLGA-based bioabsorbable stent into the arterial wall. Fig. 3 presents pressure and velocity field induced by the blood flow in the arterial wall. We observe that the highest pressure corresponds to the regions entrapped between stent struts in the fibrous cap. The pressure decreases in the transversal direction. Drug release from the stent into the arterial wall during one year has been depicted in Fig. 4. Less drug concentration is observed in the boundary $\Gamma_{\text{lumen}-\text{cap}} \cup \Gamma_{\text{wall}-\text{lumen}} \cup \Gamma_{\text{cap}-\text{lumen}}$ as it is washed out by the blood flow.

Fig. 5 shows the effect of degradation rate on the drug release from the stent into the arterial wall. Depending on the ratio of lactide to glycolide used for the polymerization (copolymer ratio), PLGA with different degradation rates can be obtained [20]. Fig. 5(a) shows the degradation pattern of PLGA with different copolymer ratios. As expected PLGA vanishes faster when degradation rate is larger. In the other words to maintain the polymer for a longer time, the degradation rate of the corresponding copolymer should be decreased. Fig. 5(b) and (c) show good agreement between fluid entrance into PLGA, PLGA degradation and monomer's transport for all degradation rates. The penetration of the fluid in the polymer presents a steep initial slope and gradually achieves its steady state.

Fig. 5 (d) shows the time evolution of the mass of the dissolved drug in the polymeric stent. We observe that the mass of the dissolved drug increases with a steep initial gradient due to the conversion from the solid state to the dissolved state and then gradually decreases due to the release of the dissolved drug into the fibrous cap, described by the interface boundary conditions (15). The degradation rate of PLGA has implicit influence on the drug release profile so that increasing of the degradation rate accelerates the drug release from the stent.

Comparing Figs. 5(d) and 6 indicates that drug releases faster from the stent with a higher degradation rate and corresponds to a higher peak of the unbound drug in the arterial wall. In a longer time, degradation rate has no significant influence on the residence time of the unbound drug in the arterial wall. In the other words after six months, the amount of remained drug in the arterial wall is identical for all degradation rates.

In Fig. 7, the time evolution of the mass of the unbound and bound drugs in different regions of the arterial wall is illustrated. Fig. 7 shows that the unbound and bound drugs initially increase in the fibrous cap and then gradually decrease due to diffusion of the unbound drug into other regions of the arterial wall (plaque and healthy part). Fibrous cap is the first layer which vanishes the drug while drug in the other regions vanishes in a longer time.

4. Conclusions

In this paper, we analyzed the interplay between the main contributors of the drug release from PLGA-based drug-eluting stents: the coated stent and viscoelasticity of the arterial wall. Our main conclusions are summarized as follows:

- Polymer degradation: The vanishing time of polymer can be controlled by copolymerization ratio. The polymer vanishes faster and the monomer releases faster into different layers of the arterial wall when the degradation rate is higher (Fig. 5 (a) and (b)).

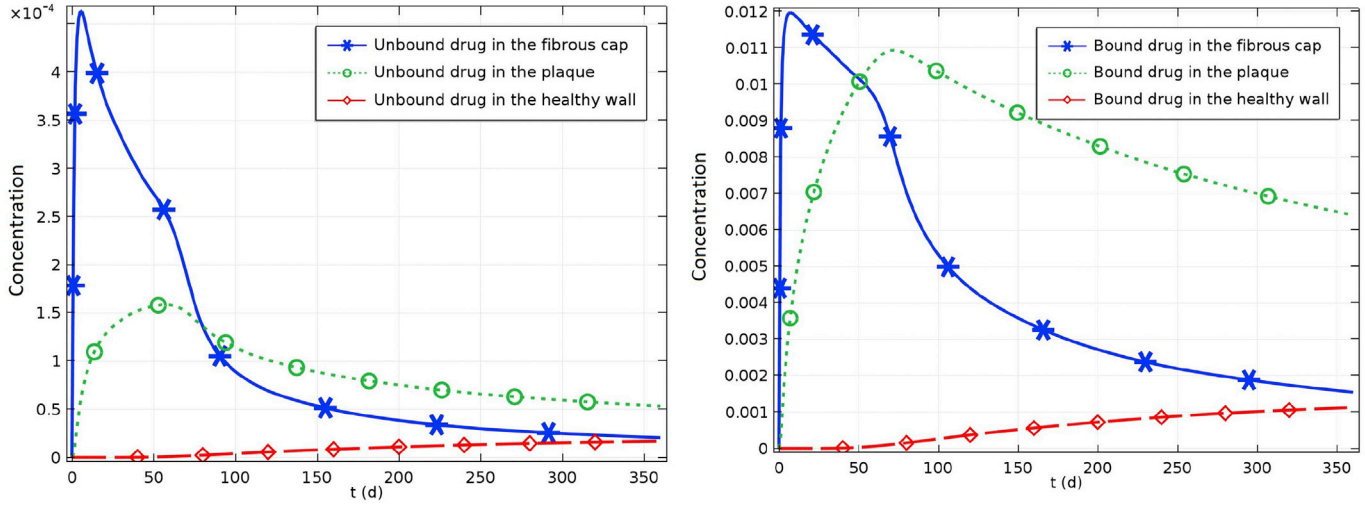

(a) Unbound drug, (b) Bound drug,

Fig. 7. Mean concentration of the unbound and bound drugs $\left[\frac{mol}{cm^2}\right]$ in the arterial wall.

- Drug distribution: Drug in a PLGA-based stent with a higher degradation rate releases faster and takes a higher peak in the arterial wall but in a long time, degradation rate has no significant influence on the residence time of the drug in the arterial wall (Fig. 5 (d) and Fig. 6).
- Drug accumulation in the arterial wall: Unbound and bound drugs initially increase in the fibrous cap and then gradually decrease due to the transfer of the unbound drug from the fibrous cap to other regions of the arterial wall (Fig. 7).

Although cardiovascular delivery depends on many other biochemical and physiological phenomena that have not been considered in this paper, we believe that our results can pave the way for a future design of a predictive tool in the follow-up of stented patients.

Conflict of interest statement

The authors declare that no conflict of interest occurs.

Acknowledgements

This work is supported by Alexander von Humboldt Foundation (AvH) under the Georg Forster Research Fellowship (HERMES) and hosted by Institute of Structural Mechanics (ISM), Bauhaus-Universität Weimar.

References

[1] I. Pericevic, C. Lally, D. Toner, D.J. Kelly, The influence of plaque composition on underlying arterial wall stress during stent expansion: the case for lesion-specific stents, Med. Eng. Phys. 31 (4) (2009) 428–433.
[2] Y. Huang, H.C.A. Ng, X.W. Ng, V. Subbu, Drug-eluting biostable and erodible stents, J. Control. Release 193 (2014) 188–201.
[3] Y. Wang, X. Lou, X. Xu, J. Zhu, Y. Shang, Drug-eluting balloons versus drug-eluting stents for the management of in-stent restenosis: a meta-analysis of randomized and observational studies, J. Cardiol. (Mar 2017), http://dx.doi.org/10.1016/j.jjcc.2016.12.019.
[4] Y. Nishimoto, Y. Ueda, R. Sugihara, A. Murakami, K. Ueno, Y. Takeda, A. Hirata, K. Kashiwase, Y. Higuchi, Y. Yasumura, Comparison of angioscopic findings among second-generation drug-eluting stents, J. Cardiol. 70 (Sep 2017) 297–302.
[5] A. Omar, L.K. Pendyala, J.A. Ormiston, R. Waksman, Review: stent fracture in the drug-eluting stent era, Cardiovasc. Revascularization Med. 17 (Sep 2016) 404–411.
[6] W. Khan, S. Farah, A.J. Domb, Drug eluting stents: developments and current status, J. Control. Release 161 (Jul 2012) 703–712.
[7] G.A.A. Holzapfel, T.C. Gasser, R.W. Ogden, A new constitutive framework for arterial wall mechanics and a comparative study of material models, J. Elast. (2000) 1–48.
[8] F. Bozsak, J.-M. Chomaz, A.I. Barakat, Modeling the transport of drugs eluted from stents: physical phenomena driving drug distribution in the arterial wall, Biomech. Model. Mechanobiol. 13 (Apr 2014) 327–347.
[9] S. Prabhu, S. Hossainy, Modeling of degradation and drug release from a biodegradable stent coating, J. Biomed. Mater. Res. A 80 (Mar 2007) 732–741.
[10] G. Pontrelli, F. de Monte, A multi-layer porous wall model for coronary drug-eluting stents, Int. J. Heat Mass Transf. 53 (Sep 2010) 3629–3637.
[11] P. Zunino, Multidimensional pharmacokinetic models applied to the design of drug eluting stents, Cardiov. Eng. 4 (2) (Jun 2004) 181–191.
[12] X. Zhu, R.D. Braatz, Modeling and analysis of drug-eluting stents with biodegradable PLGA coating: consequences on intravascular drug delivery, J. Biomech. Eng. 136 (11) (2014) 111004.
[13] G. Vairo, M. Cioffi, R. Cottone, G. Dubini, F. Migliavacca, Drug release from coronary eluting stents: a multidomain approach, J. Biomech. 43 (8) (2010) 1580–1589.
[14] S. McGinty, G. Pontrelli, A general model of coupled drug release and tissue absorption for drug delivery devices, J. Control. Release 217 (2015) 327–336.
[15] S. McGinty, A decade of modelling drug release from arterial stents, Math. Biosci. 257 (Nov 2014) 80–90.
[16] J.A. Ferreira, J. Naghipoor, P.D. Oliveira, A coupled non-Fickian model of a cardiovascular drug delivery system, Math. Med. Biol. 275 (Jul 2015) 1–29.
[17] J. Naghipoor, J.A. Ferreira, P. de Oliveira, T. Rabczuk, Tuning polymeric and drug properties in a drug eluting stent: a numerical study, Appl. Math. Model. 40 (Sep 2016) 8067–8086.
[18] J.A. Ferreira, L. Gonçalves, J. Naghipoor, P. de Oliveira, T. Rabczuk, The influence of atherosclerotic plaques on the pharmacokinetics of a drug eluted from bioabsorbable stents, Math. Biosci. 283 (Jan 2017) 71–83.
[19] N. Foin, R.D. Lee, R. Torii, J.L. Guitierrez-Chico, A. Mattesini, S. Nijjer, S. Sen, R. Petraco, J.E. Davies, C. Di Mario, M. Joner, R. Virmani, P. Wong, Impact of stent strut design in metallic stents and biodegradable scaffolds, Int. J. Cardiol. 177 (3) (2014) 800–808.
[20] G. Mani, M.D. Feldman, D. Patel, C.M. Agrawal, Coronary stents: a materials perspective, Biomaterials 28 (Mar 2007) 1689–1710.
[21] A.N. Ford Versypt, D.W. Pack, R.D. Braatz, Mathematical modeling of drug delivery from autocatalytically degradable PLGA microspheres–a review, J. Control. Release 165 (1) (2013) 29–37.
[22] X. Zhu, R.D. Braatz, A mechanistic model for drug release in PLGA biodegradable stent coatings coupled with polymer degradation and erosion, J. Biomed. Mater. Res. Part A 103 (7) (2015) 2269–2279.
[23] M. Grassi, G. Grassi, Mathematical modeling and controlled drug delivery: matrix systems, Curr. Drug Deliv. 2 (4) (2005) 97–116.
[24] F. Rossi, T. Casalini, E. Raffa, M. Masi, G. Perale, E. Ra, M. Masi, G. Perale, E. Raffa, M. Masi, G. Perale, Bioresorbable polymer coated drug eluting stent: a model study, Mol. Pharm. 9 (Jul 2012) 1898–1910.
[25] G. Perale, P. Arosio, D. Moscatelli, V. Barri, M. Müller, S. Maccagnan, M. Masi, A new model of resorbable device degradation and drug release: transient 1-dimension diffusional model, J. Control. Release 136 (3) (2009) 196–205.
[26] S. Minisini, Mathematical and Numerical Modeling of Controlled Drug Release, Phd thesis, Politecnico di Milano, 2009.
[27] A. Borghi, E. Foa, R. Balossino, F. Migliavacca, G. Dubini, Modelling drug elution from stents: effects of reversible binding in the vascular wall and degradable polymeric matrix, Comput. Methods Biomech. Biomed. Engin. 11 (Aug 2008) 367–377.
[28] J.A. Ferreira, J. Naghipoor, P. de Oliveira, The effect of reversible binding sites on drug release from drug eluting stents, in: Proceeding 14th Int. Conf. Math. Methods Sci. Eng, 2015, pp. 519–530.
[29] A. Nekouzadeh, K.M. Pryse, E.L. Elson, G.M. Genin, A simplified approach to quasi-linear viscoelastic modeling, J. Biomech. 40 (Jan 2007) 3070–3078.
[30] Y. Tao, Nonlinear Viscoelastic Properties and Constitutive Modeling of Blood Vessel, Master thesis, National University of Singapore, 2009.
[31] Y.C. Fung, Biomechanics Mechanical Properties of Living Tissues. Biomechanics/Y. C. Fung, Springer-Verlag, 1981.
[32] H.F. Brinson, L.C. Brinson, Polymer Engineering Science and Viscoelasticity: an Introduction, Springer, 2010.
[33] A.R. Tzafriri, A.D. Levin, E.R. Edelman, Diffusion-limited binding explains binary dose response for local arterial and tumour drug delivery, Cell Prolif. 42 (Jun 2009) 348–363.
[34] S. McGinty, M. Wheel, S. McKee, C. McCormick, Does anisotropy promote spatial uniformity of stent-delivered drug distribution in arterial tissue? Int. J. Heat Mass Transf. 90 (2015) 266–279.
[35] F. Bozsak, D. Gonzalez-Rodriguez, Z. Sternberger, P. Belitz, T. Bewley, J.-M.M. Chomaz, A.I. Barakat, Optimization of drug delivery by drug-eluting stents, PLoS One 10 (Jun 2015), e0130182.
[36] M. D'Errico, P. Sammarco, G. Vairo, Analytical modeling of drug dynamics induced by eluting stents in the coronary multi-layered curved domain, Math. Biosci. 267 (2015) 79–96.